

Appendix A

Statistical Synopsis

for the 2002 Fixed-Location Hydroacoustic Investigations

at The Dalles Dam

Prepared for:

Gary E. Johnson
Battelle Pacific Northwest Division
Richland WA 99352

Prepared by:

John R. Skalski
Columbia Basin Research
School of Aquatic and Fishery Sciences
University of Washington
1325 Fourth Avenue, Suite 1820
Seattle, Washington 98101

4 June 2002

Appendix A

Statistical Synopsis for the 2002 Fixed-Location Hydroacoustic Investigations at The Dalles Dam

The purpose of this synopsis is to describe the statistical methods to be used in the analysis of the 2002 hydroacoustic study at The Dalles Dam. The study will estimate fish passage through the powerhouse (i.e., turbines), spillway, fish units, and sluiceway during the spring smolt outmigration. These estimates of fish passage will be used to estimate various measures of spillbay and sluiceway passage performance at The Dalles Dam. The spillway and sluiceway performance measures will be used to test the effect of the J-occlusion plates at turbine units 1-4 on diverting smolts from the turbine intakes at The Dalles Dam.

A.1 Transducer Deployment and Sampling Scheme

This section describes the hydroacoustic sampling schemes that were used to estimate smolt passage at the powerhouse, spillway, sluiceway, and fish units at The Dalles Dam.

A.1.1 Sampling at Powerhouse

The Dalles powerhouse has 22 turbine units, each with 3 turbine intake slots. The turbine units selected for hydroacoustic monitoring and the number of intake slots per unit sampled varied considerably across the project in 2002.

The selected intake slots were sampled 24 hrs daily throughout the study period. Within an hour at an intake slot, fish passage was systematically sampled over time. The sampling effort within an hour at the various intake slots is summarized in Table A.1. Table A.2 summarizes the transducer deployment and the post-hoc grouping of turbine units into statistical strata.

Table A.1. Sampling Effort for each hour for Turbine Units 1 through 22

Turbine Units	Sampling Effort
1-7	10 1-min samples/hr
8-22	6 1-min samples/hr

Table A 2. Summary of Transducer Deployment at Turbine Units 1-22 at The Dalles Dam in 2002. Number of intakes sampled per unit is given along with the *post-hoc* grouping of units into statistical strata and the number of intakes sampled per stratum.

Unit	1	2	3	4	5	6	7	8	9	10	11	12	13	14	15	16	17	18	19	20	21	22
Transducer/Unit	1/3	2/3	2/3	2/3	1/3	1/3	1/3	1/3	0/3	0/3	1/3	1/3	1/3	1/3	0/3	1/3	1/3	0/3	1/3	0/3	1/3	0/3
Strata	1	1	2	3	4	4	5	5	5	6	6	6	7	7	8	8	8	9	9	9	9	9
Transducer/Stratum	3/6		2/3	2/3	2/6			2/9			2/9		2/6		2/9					2/15		

A.1.2 Sampling at Spillway

The Dalles Dam has 23 spillbays within the spillway. During 2002, only spillbays 1-15 were open during all or part of the study period. At each spillbay, a transducer was randomly located across the breadth of the opening (i.e., left, right, or center) to monitor fish passage. Hence, 15 of 15 spillbays were monitored during the study. Hydroacoustic monitoring was conducted 24 hrs daily throughout the study. Within an hour at a spillbay, fish passage was systematically sampled over time. The within-hour sampling effort varied between spillbay locations; the sampling frequency varied as follows:

- 8 1-min samples/hr,
- 10 1-min samples/hr, or
- 30 1-min samples/hr.

A.1.3 Sampling at Fish Units

There are two fish units at The Dalles Dam, each with two intakes. During the 2002 study, 1 of 2 intake slots was randomly selected for hydroacoustic monitoring. The selected intakes were sampled 24 hrs daily throughout the study period. Within an hour at an intake slot, fish passage was systematically sampled over time. The sampling effort within an hour at each intake slot was 10 1-min samples/hr.

A.1.4 Sampling at Sluiceway

Two different approaches will be used to sample smolt passage in the sluiceway depending on whether the J-occlusion plates are installed or not. When the J-plates are installed, a single uplooking transducer will monitor smolt passage at sluiceway 1-2. When the J-plates are not installed (i.e., unoccluded), a single uplooking transducer will monitor smolt passage at each of the entrances to 1-1, 1-2, and 1-3. The sampling interval within an hour will vary over time and between locations.

A.1.5 Sampling in Forebay

One split-beam transducer will be located at the pier-nose between turbine units 3 and 4. The orientation of the transducer will be changed between test blocks. The transducer orientation will be changed systematically between test blocks from a vertical to a horizontal position (i.e., Block 1 – horizontal, Block 2 – vertical, Block 3 – horizontal, etc.). The transducer will sample continuously; all 60 min per hr, 24 hr/day.

A.2 Estimating Fish Passage

The following sections describe how the estimates of smolt passage will be calculated at the various locations at The Dalles Dam.

A.2.1 Powerhouse Passage

The sampling at The Dalles powerhouse turbines can be envisioned as a stratified two-stage sampling program. Constructing spatial strata by combining adjacent turbine units, the first step was the random sampling of turbine intake slots within adjacent turbine units. Table A.1 summarizes the nine spatial strata constructed and the numbers of intake slots sampled per stratum.

The estimator of total turbine passage over the course of D days can be expressed as follows

$$\hat{T} = \sum_{i=1}^D \sum_{j=1}^{24} \sum_{k=1}^K \left[\frac{A_k}{a_k} \left[\sum_{l=1}^{a_k} \hat{T}_{ijkl} \right] \right] \quad (1)$$

where

\hat{T}_{ijkl} = estimated fish passage in the l th intake slot ($l = 1, \dots, a_k$) within the k th turbine stratum ($k = 1, \dots, K$) during the j th hour ($j = 1, \dots, 24$) on the i th day ($i = 1, \dots, D$);

a_k = number of intake slots sampled in the k th turbine stratum ($k = 1, \dots, K$);

A_k = total number of intake slots within the k th turbine stratum ($k = 1, \dots, K$);

K = number of turbine strata created (nominally $K = 9$).

The estimator of \hat{T}_{ijkl} is based on the assumption of simple random sampling within a slot-hour, in which case

$$\hat{T}_{ijkl} = \frac{B_{kl}}{b_{kl}} \sum_{g=1}^{b_{kl}} w_{ijklg} \quad (2)$$

where

w_{ijklg} = expanded fish passage in the g th sampling unit ($g = 1, \dots, b_{ijkl}$) in the l th intake slot ($l = 1, \dots, a_k$) within the k th turbine stratum ($k = 1, \dots, K$) during the j th hour ($j = 1, \dots, 24$) on the i th day ($i = 1, \dots, D$);

b_{kl} = number of sampling units per hour actually observed in the l th intake slot ($l = 1, \dots, a_k$) within the k th turbine stratum ($k = 1, \dots, K$);

B_{kl} = total number of possible sampling units per hour within the l th intake slot ($l = 1, \dots, a_k$) within the k th turbine stratum ($k = 1, \dots, K$).

Nominally, $B_{kl} = 60$ and $b_{kl} = 6$ or 10 , depending on location.

Combining Equations (1) and (2), the estimator for total powerhouse passage can be written as

$$\hat{T} = \sum_{i=1}^D \sum_{j=1}^{24} \sum_{k=1}^K \left[\frac{A_k}{a_k} \sum_{l=1}^{a_k} \frac{B_{kl}}{b_{kl}} \sum_{g=1}^{b_{kl}} w_{ijklg} \right] \quad (3)$$

The estimator for the variance of \hat{T} can be expressed as follows

$$\widehat{Var}(\hat{T}) = \sum_{i=1}^D \sum_{j=1}^{24} \sum_{k=1}^K \left[\frac{A_k^2 \left(1 - \frac{a_k}{A_k} \right) s_{\hat{T}_{ijk}}^2}{a_k} + \frac{A_k \sum_{l=1}^{a_k} \widehat{Var}(\hat{T}_{ijkl})}{a_k} \right] \quad (4)$$

where

$$s_{\hat{T}_{ijk}}^2 = \frac{\sum_{l=1}^{a_k} \left(\hat{T}_{ijkl} - \hat{\bar{T}}_{ijk} \right)^2}{(a_k - 1)},$$

$$\hat{\bar{T}}_{ijk} = \frac{1}{a_k} \sum_{l=1}^{a_k} \hat{T}_{ijkl},$$

and where

$$\widehat{Var}(\hat{T}_{ijkl}) = \frac{B_{kl}^2 \left(1 - \frac{b_{kl}}{B_{kl}}\right) s_{w_{ijkl}}^2}{b_{kl}},$$

$$s_{w_{ijkl}}^2 = \frac{\sum_{g=1}^{b_{kl}} (w_{ijklg} - \bar{w}_{ijkl})^2}{(b_{kl} - 1)},$$

$$\bar{w}_{ijkl} = \frac{1}{b_{kl}} \sum_{g=1}^{b_{kl}} w_{ijklg}.$$

A.2.2 Spillway Passage

The sampling at The Dalles spillway can be envisioned as stratified random sampling within spillbay-hours, in which case, total spillway passage over D days can be estimated by the formula

$$\widehat{SP} = \sum_{i=1}^D \sum_{j=1}^{24} \sum_{k=1}^{15} \left[\frac{C_{ijk}}{c_{ijk}} \sum_{l=1}^{c_{ijk}} x_{ijkl} \right] \quad (5)$$

where

x_{ijkl} = expanded fish passage in the l th sampling interval ($l = 1, \dots, t_{ijk}$) during the j th hour ($j = 1, \dots, 24$) at the k th spillbay ($k = 1, \dots, 15$) on the i th day ($i = 1, \dots, D$);

C_{ijk} = total number of possible sampling units within the j th hour ($j = 1, \dots, 24$) at the k th spillbay ($k = 1, \dots, 15$) on the i th day ($i = 1, \dots, D$);

c_{ijk} = number of sampling units actually observed within the j th hour ($j = 1, \dots, 24$) at the k th spillbay ($k = 1, \dots, 15$) on the i th day ($i = 1, \dots, D$).

Nominally, $C_{ijk} = 60$ and $c_{ijk} = 8, 10, \text{ or } 30$.

The estimator for the variance of \widehat{SP} can be expressed as follows

$$\widehat{Var}(\widehat{SP}) = \sum_{i=1}^D \sum_{j=1}^{24} \sum_{k=1}^{14} \left[\frac{C_{ijk}^2 \left(1 - \frac{c_{ijk}}{C_{ijk}} \right) S_{x_{ijk}}^2}{c_{ijk}} \right] \quad (6)$$

where

$$S_{x_{ijk}}^2 = \frac{\sum_{l=1}^{c_{ijk}} (x_{ijkl} - \bar{x}_{ijk})^2}{(c_{ijk} - 1)}$$

and where

$$\bar{x}_{ijk} = \frac{1}{c_{ijk}} \sum_{l=1}^{c_{ijk}} x_{ijkl} .$$

A.2.3 Fish Unit Passage

The sampling at The Dalles fish units can be envisioned as a stratified two-stage sampling program. The first stage is the random sampling of 2 of 4 intake slots across the two fish units. In the second stage, slot-hours are treated as strata, and random sampling within slot-hours is performed, in which case, total fish unit passage can be estimated by the formula

$$\hat{F} = \frac{4}{2} \sum_{i=1}^D \sum_{j=1}^{24} \sum_{k=1}^2 \left[\frac{M}{m} \sum_{l=1}^m z_{ijkl} \right] \quad (7)$$

where

z_{ijkl} = expanded fish count in the l th sampling interval ($l = 1, \dots, m$) during the j th hour ($j = 1, \dots, 24$) at the k th fish unit slot ($k = 1, 2$) on the i th day ($i = 1, \dots, D$);

M = total number of possible sampling units within the j th hour ($j = 1, \dots, 24$) at the k th fish unit slot ($k = 1, 2$) on the i th day ($i = 1, \dots, D$);

m = number of sampling units actually observed within the j th hour ($j = 1, \dots, 24$) at the k th fish unit slot ($k = 1, 2$) on the i th day ($i = 1, \dots, D$).

Nominally, $M = 60$ and $m = 10$.

The estimator for the variance of \hat{F} can be expressed as follows

$$\widehat{Var}(\hat{F}) = \frac{\sum_{i=1}^D \sum_{j=1}^{24} \left[\frac{4^2 \left(1 - \frac{2}{4}\right) s_{\hat{F}_{ijk}}^2}{2} \right]}{2} + \frac{4 \sum_{i=1}^D \sum_{j=1}^{24} \sum_{k=1}^2 \left[\frac{M^2 \left(1 - \frac{m}{M}\right) s_{z_{ijk}}^2}{m} \right]}{2} \quad (8)$$

where

$$s_{z_{ijk}}^2 = \frac{\sum_{l=1}^m (z_{ijkl} - \bar{z}_{ijk})^2}{(m-1)},$$

$$\bar{z}_{ijk} = \frac{1}{m} \sum_{l=1}^m z_{ijkl},$$

and where

$$s_{\hat{F}_{ijk}}^2 = \frac{\sum_{k=1}^2 (\hat{F}_{ijk} - \hat{\bar{F}}_{ij})^2}{(2-1)},$$

$$\hat{\bar{F}}_{ij} = \frac{1}{2} \sum_{k=1}^2 \hat{F}_{ijk},$$

$$\hat{F}_{ijk} = \frac{M}{m} \sum_{l=1}^m z_{ijkl}.$$

A.2.4 Sluiceway Passage

The estimation of sluiceway passage will differ whether the J-occlusion plates are installed or not. The subsequent sections describe the estimation under both test conditions. With only one of three sluiceway entrances monitored, estimation of total sluiceway passage must be based on expanding the observed counts to all three passage routes. The estimator of total sluiceway passage in this case can be expressed as follows:

$$\widehat{SL} = 3 \sum_{i=1}^D \sum_{j=1}^{24} \left[\frac{N_{ij}}{n_{ij}} \sum_{l=1}^{n_{ij}} y_{ijl} \right] \quad (9)$$

where

y_{ijl} = expanded fish count in the l th sampling interval ($l = 1, \dots, m$) during the j th hour ($j = 1, \dots, 24$) on the i th day ($i = 1, \dots, D$);

N_{ij} = total number of possible sampling units within the j th hour ($j = 1, \dots, 24$) of the i th day ($i = 1, \dots, D$);

n_{ij} = number of sampling units actually observed within the j th hour ($j = 1, \dots, 24$) of the i th day ($i = 1, \dots, D$).

The estimator for the variance of (9) can be expressed as follows:

$$\widehat{Var}(\widehat{SL}) = 9 \sum_{i=1}^D \sum_{j=1}^{24} \frac{N_{ij}^2 \left(1 - \frac{n_{ij}}{N_{ij}}\right) s_{y_{ij}}^2}{n_{ij}} \quad (10)$$

where

$$s_{y_{ij}}^2 = \frac{\sum_{l=1}^{n_{ij}} (y_{ijl} - \bar{y}_{ij})^2}{(n_{ij} - 1)},$$

$$\bar{y}_{ij} = \frac{\sum_{l=1}^{n_{ij}} y_{ijl}}{n_{ij}}.$$

Variance formula (10) will likely underestimate the true variance because it does not take into account the variation in smolt passage between entrances.

When the J-occlusion plates are not installed, all three of the sluiceway entrances will be hydroacoustically monitored. The estimate of total sluiceway passage can then be estimated as follows:

$$\widehat{SL} = \sum_{i=1}^D \sum_{j=1}^{24} \sum_{k=1}^3 \left[\frac{N_{ijk}}{n_{ijk}} \sum_{l=1}^{n_{ijk}} y_{ijkl} \right] \quad (11)$$

where

y_{ijkl} = expanded fish count in the l th sampling interval ($l = 1, \dots, n_{ijk}$) during the j th hour ($j = 1, \dots, 24$) on the i th day ($i = 1, \dots, D$) at the k th sluiceway entrance;

N_{ijk} = total number of possible sampling units within the j th hour ($j = 1, \dots, 24$) on the i th day ($i = 1, \dots, D$) at the k th sluiceway entrance ($k = 1, \dots, 3$);

n_{ijk} = number of sampling units actually observed within the j th hour ($j = 1, \dots, 24$) on the i th day ($i = 1, \dots, D$) at the k th sluiceway entrance ($k = 1, \dots, 3$).

The estimator for the variance of \widehat{SL} can be expressed as follows

$$\widehat{Var}(\widehat{SL}) = \sum_{i=1}^D \sum_{j=1}^{24} \sum_{k=1}^3 \left[\frac{N_{ijk}^2 \left(1 - \frac{n_{ijk}}{N_{ijk}} \right) s_{y_{ijk}}^2}{n_{jk}} \right] \quad (12)$$

where

$$s_{y_{ijk}}^2 = \frac{\sum_{l=1}^{n_{ijk}} (y_{ijkl} - \bar{y}_{ijk})^2}{(n_{ijk} - 1)},$$

$$\bar{y}_{ijk} = \frac{\sum_{l=1}^{n_{ijk}} y_{ijkl}}{n_{ijk}}.$$

A.3 Estimating Passage Performance

A.3.1 Fish Passage Efficiency (FPE)

The fish passage efficiency (FPE) at The Dalles Dam will be estimated by the quotient

$$\widehat{FPE} = \frac{\widehat{SP} + \widehat{SL}}{\widehat{SP} + \widehat{SL} + \widehat{T} + \widehat{F}} \quad (13)$$

where

\widehat{SP} = estimated fish passage through the spillway,

\widehat{SL} = estimated fish passage through the sluiceway,

\widehat{T} = estimated fish passage through the turbine units,

\widehat{F} = estimated fish passage through the fish units,

and where the numerator is the estimated spillway and sluiceway passage and the denominator is the total project passage. The estimate of FPE can alternatively be expressed as

$$\widehat{FPE} = \frac{\widehat{G}}{\widehat{G} + \widehat{U}}$$

where

$$\widehat{G} = \widehat{SP} + \widehat{SL},$$

$$\widehat{U} = \widehat{T} + \widehat{F}.$$

The estimator for the variance of \widehat{FPE} can then be expressed as

$$\widehat{Var}(\widehat{FPE}) = \widehat{FPE}^2 (1 - \widehat{FPE})^2 \left[\frac{\widehat{Var}(\widehat{G})}{\widehat{G}^2} + \frac{\widehat{Var}(\widehat{U})}{\widehat{U}^2} \right] \quad (14)$$

where

$$\widehat{Var}(\widehat{G}) = \widehat{Var}(\widehat{SP}) + \widehat{Var}(\widehat{SL}),$$

$$\widehat{Var}(\widehat{U}) = \widehat{Var}(\widehat{T}) + \widehat{Var}(\widehat{F}).$$

A.3.2 Spill Efficiency (SPY)

Spill efficiency (SPY) at The Dalles Dam will be estimated by the quotient

$$\widehat{SPY} = \frac{\widehat{SP}}{\widehat{SP} + \widehat{SL} + \widehat{T} + \widehat{F}} \quad (15)$$

where the numerator is the estimate of spillway passage and the denominator is the estimate of total project passage. In turn, \widehat{SPY} can be reexpressed as

$$\widehat{SPY} = \frac{\widehat{SP}}{\widehat{SP} + \widehat{U}_1}$$

where

$$\widehat{U}_1 = \widehat{SL} + \widehat{T} + \widehat{F}.$$

The estimator for the variance of \widehat{SPY} can then be expressed as

$$\widehat{Var}(\widehat{SPY}) = \widehat{SPY}^2 (1 - \widehat{SPY})^2 \left[\frac{\widehat{Var}(\widehat{SP})}{\widehat{SP}^2} + \frac{\widehat{Var}(\widehat{U}_1)}{\widehat{U}_1^2} \right] \quad (16)$$

where

$$\widehat{Var}(\widehat{U}_1) = \widehat{Var}(\widehat{SL}) + \widehat{Var}(\widehat{T}) + \widehat{Var}(\widehat{F}).$$

A.3.3 Sluiceway Efficiency (SLY)

Sluiceway efficiency (SLY) at The Dalles Dam will be estimated by the quotient

$$\widehat{SLY} = \frac{\widehat{SL}}{\widehat{SP} + \widehat{SL} + \widehat{T} + \widehat{TF}} \quad (17)$$

where the numerator is the estimate of sluiceway passage and the denominator is the estimate of total project passage. In turn, \widehat{SLY} can be expressed as

$$\widehat{SLY} = \frac{\widehat{SL}}{\widehat{SP} + \widehat{U}_2}$$

where

$$\widehat{U}_2 = \widehat{SP} + \widehat{T} + \widehat{F}.$$

The estimator for the variance of \widehat{SLY} can then be expressed as

$$\widehat{Var}(\widehat{SLY}) = \widehat{SLY}^2 (1 - \widehat{SLY})^2 \left[\frac{\widehat{Var}(\widehat{SL})}{\widehat{SL}^2} + \frac{\widehat{Var}(\hat{U}_2)}{\hat{U}_2^2} \right] \quad (18)$$

where

$$\widehat{Var}(\hat{U}_2) = \widehat{Var}(\widehat{SP}) + \widehat{Var}(\hat{T}) + \widehat{Var}(\hat{F}).$$

A.3.4 Conditional Sluiceway Efficiency (CSLY)

The conditional probability of a smolt going through the sluiceway given it is passing through the powerhouse can be estimated by the quotient

$$\widehat{CSLY} = \frac{\widehat{SL}}{\widehat{SL} + \hat{T} + \hat{F}} \quad (19)$$

or equivalently

$$\widehat{CSLY} = \frac{\widehat{SL}}{\widehat{SL} + \hat{U}_3}$$

where

$$\hat{U}_3 = \hat{T} + \hat{F}.$$

The estimator for the variance of \widehat{CSLY} can then be expressed as follows

$$\widehat{Var}(\widehat{CSLY}) = \widehat{CSLY}^2 (1 - \widehat{CSLY})^2 \left[\frac{\widehat{Var}(\widehat{SL})}{\widehat{SL}^2} + \frac{\widehat{Var}(\hat{U}_3)}{\hat{U}_3^2} \right] \quad (20)$$

where

$$\widehat{Var}(\hat{U}_3) = \widehat{Var}(\hat{T}) + \widehat{Var}(\hat{F}).$$

A.3.5 Sluiceway Passage to Turbines 1-4 Passage

Another localized measure of sluiceway efficiency is relative to fish passage through turbine units 1-4 and is defined as

$$\widehat{SLY}_{1-4} = \frac{\widehat{SL}}{\widehat{SL} + \hat{T}_{1-4}} \quad (21)$$

where

\hat{T}_{1-4} = estimated fish passage through turbine units 1-4.

The estimator for the variance of \widehat{SLY}_{1-4} can be expressed as follows

$$\widehat{Var}(\widehat{SLY}_{1-4}) = \widehat{SLY}_{1-4}^2 (1 - \widehat{SLY}_{1-4})^2 \left[\frac{\widehat{Var}(\widehat{SL})}{\widehat{SL}^1} + \frac{\widehat{Var}(\hat{T}_{1-4})}{\hat{T}_{1-4}^2} \right]. \quad (22)$$

A.3.6 Fish Passage Effectiveness (FPN)

Fish passage effectiveness (FPN) will be estimated by the function

$$\begin{aligned} \widehat{FPN} &= \frac{\left(\frac{\widehat{SP} + \widehat{SL}}{f_{SP} + f_{SL}} \right)}{\left(\frac{\widehat{SP} + \widehat{SL} + \hat{T} + \hat{F}}{f_{SP} + f_{SL} + f_T + f_F} \right)} \\ &= \left(\frac{f}{f_{SP} + f_{SL}} \right) \cdot \widehat{FPE} \end{aligned} \quad (23)$$

where

f_{SP} = spillway flow volume,

f_{SL} = sluiceway flow volume,

f_T = turbine flow volume,

f_F = fish unit flow volume,

$$f = f_{SP} + f_{SL} + f_T + f_F.$$

The estimator for the variance of \widehat{FPN} can be expressed as follows

$$\widehat{Var}(\widehat{FPN}) = \left(\frac{f}{f_{SP} + f_{SL}} \right)^2 \cdot \widehat{Var}(\widehat{FPE}). \quad (24)$$

A.3.7 Spill Effectiveness (SPN)

Spill effectiveness (SPN) at The Dalles Dam will be estimated by the function

$$\widehat{SPN} = \frac{\left(\frac{\widehat{SP}}{f_{SP}} \right)}{\left[\frac{(\widehat{SP} + \widehat{SL} + \widehat{T} + \widehat{F})}{f} \right]} = \left(\frac{f}{f_{SP}} \right) \cdot \widehat{SPY}. \quad (25)$$

The variance of \widehat{SPN} can be estimated by the quantity

$$\widehat{Var}(\widehat{SPN}) = \left(\frac{f}{f_{SP}} \right)^2 \cdot \widehat{Var}(\widehat{SPY}). \quad (26)$$

A.3.8 Sluiceway Effectiveness (SLN)

Sluiceway Effectiveness (SLN) will be estimated by the function

$$\widehat{SLN} = \frac{\left(\frac{\widehat{SL}}{f_{SL}} \right)}{\left[\frac{(\widehat{SL} + \widehat{SP} + \widehat{T} + \widehat{F})}{f} \right]} \quad (27)$$

where

f_{SL} = sluiceway flow volume.

The estimator of SLN can be rewritten as

$$\widehat{SLN} = \left(\frac{f}{f_{SL}} \right) \cdot \widehat{SLY} \quad (28)$$

with an associated variance estimator of

$$\widehat{Var}(\widehat{SLN}) = \left(\frac{f}{f_{SL}} \right)^2 \cdot \widehat{Var}(\widehat{SLY}). \quad (29)$$

A.3.9 Conditional Sluiceway Effectiveness (CSLN)

Conditional sluiceway effectiveness (\widehat{CSLN}) will be estimated by the quantity

$$\begin{aligned} \widehat{CSLN} &= \frac{\left(\frac{\widehat{SL}}{f_{SL}} \right)}{\left(\frac{\widehat{SL} + \widehat{T} + \widehat{F}}{f_{SL} + f_T + f_F} \right)} \\ &= \left(\frac{f_{SL} + f_T + f_F}{f_{SL}} \right) \cdot \widehat{CSLY}. \end{aligned} \quad (30)$$

The estimator for the variance of \widehat{CSLN} can then be expressed as

$$\widehat{Var}(\widehat{CSLN}) = \left(\frac{f_{SL} + f_T + f_F}{f_{SL}} \right)^2 \cdot \widehat{Var}(\widehat{CSLY}). \quad (31)$$

A.3.10 Relative Effectiveness of Sluiceway to Turbine Units 1-4 (SLN1-4)

The relative effectiveness of the sluiceway compared to turbine units 1-4 can be estimated by the quantity

$$\begin{aligned}\widehat{SLN}_{1-4} &= \frac{\left(\frac{\widehat{SL}}{f_{SL}}\right)}{\left(\frac{\widehat{SL} + \hat{T}_{1-4}}{f_{SL} + f_{1-4}}\right)} \\ &= \left(\frac{f_{SL} + f_{1-4}}{f_{SL}}\right) \cdot \widehat{SLY}_{1-4}\end{aligned}\quad (32)$$

with associated variance estimator

$$\widehat{Var}(\widehat{SLN}_{1-4}) = \left(\frac{f_{1-4}}{f_{SL}}\right)^2 \cdot \widehat{Var}(\widehat{SLY}_{1-4}) \quad (33)$$

where

f_{1-4} = flow volume through turbine units 1-4.

A.3.11 Single Turbine Unit Passage

The estimate of passage through any one turbine unit depends on whether one or two intake slots are sampled at the unit. Below estimators and associated variances are presented for estimating turbine passage for the two cases described above.

For the case where only one of three intake slots is sampled at a turbine unit, the estimate of total turbine passage can be expressed as

$$\hat{T} = 3 \sum_{i=1}^D \sum_{j=1}^{24} \frac{B}{b} \sum_{g=1}^b w_{ijg} \quad (34)$$

where

w_{ijg} = expanded fish passage in the g th sampling unit ($g = 1, \dots, b$) in the j th hour ($j = 1, \dots, 24$) of the i th day ($i = 1, \dots, D$);

b = number of sampling units per hour actually observed;

B = total number of possible sampling units per hour.

The estimator for the variance of \hat{T} can then be expressed as

$$Var(\hat{T}) = 9 \sum_{i=1}^D \sum_{j=1}^{24} \left[\frac{B^2 \left(1 - \frac{b}{B}\right) s_{w_{ij}}^2}{b} \right] \quad (35)$$

where

$$s_{w_{ij}}^2 = \frac{\sum_{g=1}^b (w_{ijg} - \bar{w}_{ij})^2}{(b-1)},$$

$$\bar{w}_{ij} = \frac{\sum_{g=1}^b w_{ijg}}{b}.$$

The variance estimator (35) will tend to underestimate the true sampling error for it ignores the between-slot variance component that cannot be estimated when only one of three slots are surveyed.

For turbine units where two of three intake slots are sampled, the estimate of total turbine passage can be expressed as

$$\hat{T} = \sum_{i=1}^D \sum_{j=1}^{24} \frac{3}{2} \sum_{l=1}^2 w_{ijlg} \quad (36)$$

where

w_{ijlg} = expanded fish passage in the g th sampling unit ($g = 1, \dots, b_l$) in the j th hour ($j = 1, \dots, 24$) of the i th day ($i = 1, \dots, D$) at the l th intake slot ($l = 1, 2$);

b_l = number of sampling units per hour actually observed at the l th intake slot ($l = 1, 2$);

B_l = total number of possible sampling units per hour at the l th intake slot ($l = 1, 2$).

The estimator for the variance of \hat{T} (Equation 36) can then be expressed as follows:

$$\widehat{Var}(\hat{T}) = \sum_{i=1}^D \sum_{j=1}^{24} \left[\frac{3^2 \left(1 - \frac{2}{3}\right) s_{\hat{T}_{ij}}^2}{2} + \frac{3 \sum_{l=1}^2 \widehat{Var}(\hat{T}_{ijl})}{2} \right] \quad (37)$$

where

$$s_{\hat{T}_{ij}}^2 = \frac{\sum_{l=1}^2 (\hat{T}_{ijl} - \hat{\bar{T}}_{ij})^2}{(2-1)},$$

$$\hat{T}_{ijl} = \frac{B_l}{b_l} \sum_{g=1}^{b_l} w_{ijlg},$$

$$\hat{\bar{T}}_{ij} = \frac{\sum_{l=1}^2 \hat{T}_{ijl}}{2}$$

and where

$$\widehat{Var}(\hat{T}_{ijl}) = \frac{B^2 \left(1 - \frac{b}{B}\right) s_{w_{ijl}}^2}{b},$$

$$s_{w_{ijl}}^2 = \frac{\sum_{g=1}^{b_l} (w_{ijlg} - \bar{w}_{ijl})^2}{(b_l - 1)},$$

$$\bar{w}_{ijl} = \frac{\sum_{g=1}^{b_l} w_{ijlg}}{b_l}.$$

A.3.12 Passage through Turbine Units 1-4

An estimate of total smolt passage through turbine units 1-4 is a special case of Estimator (3) where only the first three strata are considered (see Table A.2). The estimator would be written as

$$\hat{T}_{1-4} = \sum_{i=1}^D \sum_{j=1}^{24} \sum_{k=1}^3 \left[\frac{A_k}{a_k} \sum_{l=1}^{a_k} \frac{B_{kl}}{b_{kl}} \sum_{g=1}^{b_{kl}} w_{ijklg} \right] \quad (38)$$

where all the quantities are defined as in Section 3.1. The variance would be calculated analogous to Equation (4) where

$$\widehat{Var}(\hat{T}_{1-4}) = \sum_{i=1}^D \sum_{j=1}^{24} \sum_{k=1}^3 \left[\frac{A_k^2 \left(1 - \frac{a_k}{A_k}\right) s_{\hat{T}_{ijk}}^2}{a_k} + \frac{A_k \sum_{l=1}^{a_k} \widehat{Var}(\hat{T}_{ijkl})}{a_k} \right] \quad (39)$$

A.4 Test of J-Occlusion Treatment Effect

A randomized block experimental design was performed at The Dalles Dam to test the effect of J-occlusion plates at turbine units 1-4. The goal of the J-occlusion plates is to reduce smolt passage through the turbine units and enhance passage through the spillway and sluiceway. Fourteen test blocks were conducted with J-occlusion plates in and out. Each trial was performed for three consecutive days (i.e., 72 hours) within a test block.

Separate analyses will be performed for the daytime and nighttime periods of the trials. Separate analyses will be performed to assess the following response variables and hypotheses:

$$\begin{array}{ll} FPE & H_o : \mu_U = \mu_O \\ & H_a : \mu_U \neq \mu_O \end{array}$$

$$\begin{array}{ll} SLY_{1-4} & H_o : \mu_U = \mu_O \\ & H_a : \mu_U \neq \mu_O \end{array}$$

$$\begin{array}{ll} MU_{1-4} & H_o : \mu_U = \mu_O \\ & H_a : \mu_U \neq \mu_O \end{array}$$

where μ_U is the mean under unoccluded (OUT) conditions and μ_O is the mean under occluded (IN) conditions.

The test of the effect of the J-occlusions will be performed using a two-way ANOVA for a randomized block experimental design. The ANOVA table will be of the form depicted in Table A.3.

Table A.3. ANOVA Table

Source	df	SS	MS	F
Total	28			
Mean	1			
Total _{Cor}	27	SSTOT		
Blocks	13	SSB		
Treatments	1	SST	MST	$F_{1,13} = \frac{MST}{MSE}$
Error	13	SSE	MSE	

The F-test from the ANOVA is a two-tailed test of no treatment effect. It is recommended that all response variables be ln-transformed before the ANOVA.

Appendix B

Sonar Tracker Methods

Appendix B

Sonar Tracker Methods

Our general approach was to intensively sample fish movements in the region immediately upstream of Unit 4-3 and outside the J-extension on Unit 4-2 at The Dalles Dam (TDA). We used an active fish tracking sonar (AFTS), commonly called a sonar tracker, to obtain fish movement data. AFTS as applied at a dam (described below) was first discussed by Hedgepeth and Condiotty (1995), and later published in BioSonics (1996), Hedgepeth et al. (1999) and Hedgepeth et al. (2000). AFTS was also a key element in the Behavioral Acoustic Tracking System that is used to track acoustic-tagged fish (Johnson et al. 1998). MacLennan and Simmonds (1992) explain split-beam hydroacoustics, a main component of AFTS.

B.1 Data Collection

B.1.1 AFTS System

The components of an AFTS system (BioSonics 1998) (Figures B.1 and B.2) include a 208 (or 201) kHz BioSonics DT4000 digital split-beam echo sounder, a 7° split-beam transducer, two high-speed stepper motors for dual-axis rotation, a controller unit, a laptop computer, a desktop computer, and cables. AFTS calibration and other technical data are in Appendix A. See Johnson et al. (2001) for an error analysis of AFTS.

AFTS is based on the principle of tracking radar. This appendix provides an algorithmic description of AFTS and a simple description follows. Once a fish was detected after the transducer was randomly aimed into the sample volume, two high-speed stepper motors aligned the axis of the digital split-beam transducer on the target. As the fish moved from ping to ping, deviation of the target from the beam axis was calculated and a predictive tracking algorithm was applied to re-aim the transducer, thereby tracking the target. The predictive tracking algorithm was a discounted least-squares fit (Brookner 1998), where the most recent velocity estimate (magnitude and direction) was weighted by unity, the next most recent by one-half, the next by one-fourth, the next by one-eighth, and so on. If no target was detected after 30 sec of pinging at a given position, the aiming angles were changed to another random position. The ping rate was approximately 10 pings/sec (pps). The echo sounder threshold was set at -60 dB on-axis. For each ping the target was tracked and data on the X, Y, and Z position of the fish relative to the transducer and target strength were recorded to disk. Fish position resolution can be inferred from the angular resolution ($\pm 0.35^\circ$). At 10 m from the transducer, this would amount to ± 6 cm, and at 1 m the error would be ± 0.6 cm.

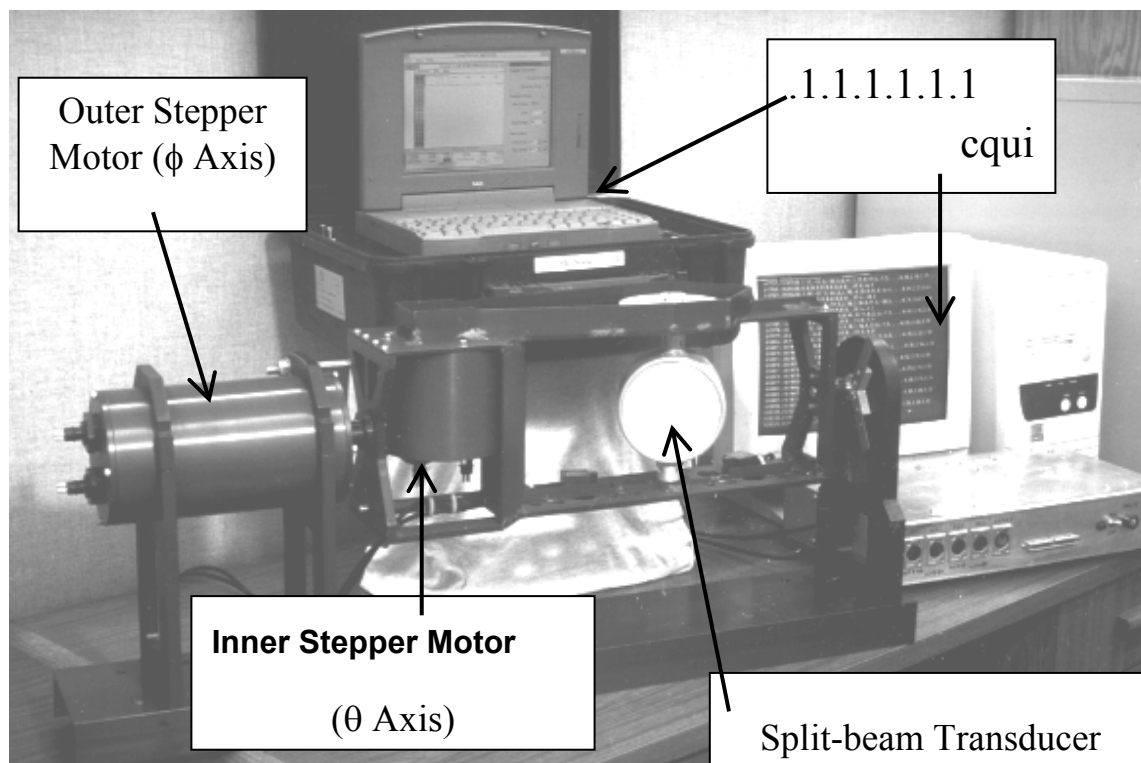


Figure B.1. Photograph of the Active Fish Tracking Sonar

Two AFTS systems were deployed at Main Unit 4. One was mounted on the tip of the J-extension at Unit 4-2 to sample fish movements on the reservoir side when the J-occlusions were in place. The other was mounted on the piernose between Main Units 4 and 5 to sample approaching fish movements when the J-occlusions were both in and out of the water. The primary area of interest for the piernose tracker was above and below the J-extension of the J-occlusion toward the east. In practice, this was limited to a region above the J-extension as described below. The primary area of interest for the J-extension tracker was 10 m above and below and 10 m into the forebay.

We calculated the position of the transducers relative to Corps of Engineers survey point TDP-1 on the pier nose at FU 2-2/MU 1-1. The location of TDP-1 was Northing 711330.743 ft, Easting 1839844.001 ft, and elevation 185 ft (Oregon State Plane N, NAD 27 horizontal datum and NGVD 29/47 vertical datum). The AFTS transducer on the J-extension of the occlusion on Main Unit 4-2 was located 91.29 m along the powerhouse 14.10 m into the forebay and -21.38 m down from TDP-1 (Northing 216887.00 m, Easting 560840.50 m and elevation 35.01 m).

The location of the AFTS transducer on the piernose between Main Units 4 and 5 was located at two levels. From May 1 to June 26 it was located 104.22 m along the powerhouse 4.43 m into the forebay and -12.04 m down from TDP-1 (Northing 216888.98 m, Easting 560856.56 m, and elevation 44.35 m). From June 28 to July 13 it was lowered about 2 m and was located 104.22 m along the powerhouse 4.91 m into the forebay and -13.96 m down from TDP-1 (Northing 216889.33 m, Easting 560856.25 m, and elevation 42.43 m).

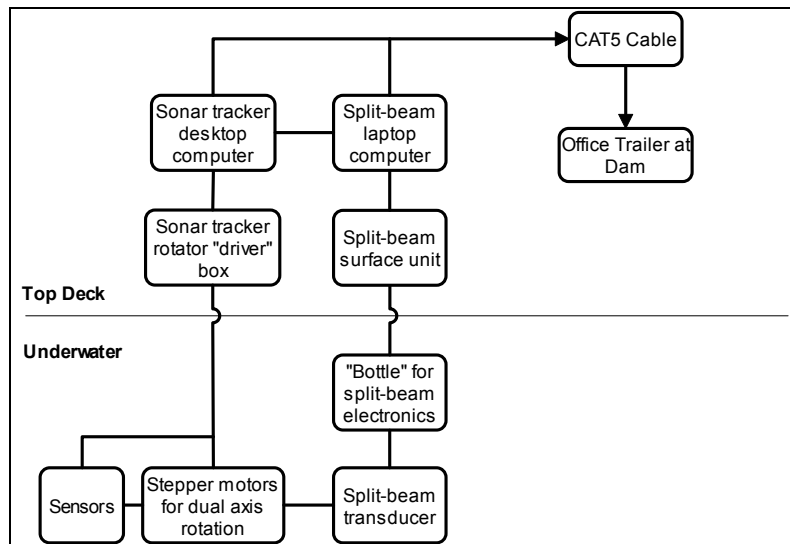


Figure B.2. Schematic Showing AFTS, with Tracker and Split-Beam Components, and Data Flow Via Network (CAT-5) Cable from an Equipment Shed at MU 4-2 to an Office Trailer at the Dam. Two of these systems were deployed.

B.1.1.1 Sample Volume of the AFTS (J-occlusion and piernose)

The decision for choosing dimensions of sampling volumes was to maximize the data used in a particular type of analysis. A Markov-chain analysis of fish tracks was the most restrictive due to the need for recording cell-to-cell movement. A fish directionality analysis was less restrictive and this approach allowed the use of all possible data. However, data from depths below 14 m at the piernose between MU 4 and 5 was not used due to noise there when J-occlusions were deployed.

B.1.1.2 Sample Volume of the J-Occlusion Tracker

With the J-occlusions IN (lowered into position), the sample volume for the sonar tracker deployed on the tip of the J-section incorporated the region in front of the J-occlusion on 4-2 from the surface to 13 m below the upper tip of the J-section and out about 13 m into the forebay (Figure B.3). Two volumes were chosen for subsequent fate movement analyses, one above and one below the level of the AFTS. The volumes' dimensions are summarized in Table B.1. Fish velocity vectors were calculated from a larger volume shown in Table B.2.

B.1.1.3 Sample Volume of the Piernose Tracker

With the J-occlusions IN and OUT, the sample volumes for the sonar tracker deployed on the piernose between Units 4 and 5 varied between two periods. This was due to operational changes made on June 28 in an attempt to establish a common and intensive sampling volume among treatments IN and OUT after that date. However, all analyses at the piernose location were constrained by the amount of noisy data below the level of the bottom of the J-occlusion extension (approximate elevation 110') observed only when the J-occlusion was deployed. The sample volume dimensions for fate of fish analyses with the J-occlusions IN and OUT are summarized in Table B.1. Sample volume dimensions were unrestricted for direction of movement analyses except that piernose AFTS data used was restricted

to depths shallower than 14 m below the surface (elevation 158') due to noisy data with J-occlusions deployed. The third set of sample volumes used in the velocity calculations are shown in Table B.2. Piernose sample volumes are shown in Figures B.4 and B.5.

Table B.1. Boundaries of the Sample Volumes by Dimension Used in Analyses of Fish Fates.

The data (in meters) are referenced to “dam coordinates” with the origin at the Intake 4-2 centerline at the plane of the piernoses at the water surface (elevation 158 ft). Positive X is to the east, positive Y is away from the dam, and positive Z is upward from the surface (negative downward in the water column).

AFTS Location	Dates		X (m)	Y (m)	Z (m)
Unit 4-2 J-Occlusion Extension	5-May to 16-June	AFTS position	0	+11.384	-13.153
		Upper Sample Volume	-6.5 to +4.5	+9.4 to +17.4	-11.5 to – 1.5
		Lower Sample Volume	-5.0 to +5.0	+12.0 to +18.0	-20.0 to – 15.0
Unit 4 – Unit 5 Piernose	1-May to 22-June	AFTS position	+12.929	+1.779	-3.658
		Sample Volume	+9.43 to +16.43	+4.1 to +9.1	-12.73 to – 5.73
	28-June to 13-July	AFTS position	+12.929	+2.1	-5.733
		Sample Volume	+12.93 to +19.93	+4.1 to +9.1	-13.73 to – 9.73

Table B.2. Boundaries of the Sample Volumes by Dimension Used in Velocity Analyses.

The data (in meters) are referenced to “dam coordinates” with the origin at the Intake 4-2 centerline at the plane of the piernoses at the water surface (elevation 158 ft). Positive X is to the east, positive Y is away from the dam, and positive Z is upward from the surface (negative downward in the water column).

AFTS Location	Dates	X (m)	Y (m)	Z (m)
Unit 4-2 J-Occlusion Extension	5-May to 16-June	-6 to +6	+10 to +20	-20 to -2
Unit 4 – Unit 5 Piernose	1-May to 22-June	+6 to +20	+4 to +11	-14 to -4
	28-June to 13-July	+13 to +23	+4 to +11	-14 to -10

B.1.2 Experimental Factors

Overall, data were collected on 7 of the possible 14 blocks using AFTS located on the J-extension at Unit 4-2 and on 12 of the 14 blocks upstream of Unit 4-3 (Table B.3). We tracked about three times as many fish in the IN condition than the OUT (Table B.3) from the piernose AFTS between Units 4 and 5. The total of ~40,000 tracked fish was slightly less than the number tracked in 2001 (Hedgepeth et al. 2002) and about half the total number tracked in the 2000 study (Johnson et al. 2001).

The experimental design for the J-occlusion evaluation called for assessing the “edge effect” of the J-occlusions. The effects of the J-occlusion were assessed by other hydroacoustic and radio telemetry

techniques in 3-day treatments (occlusions IN or OUT) randomized in 6-day blocks. Difficulties with automation programs to control sampling of AFTS early in the study resulted in lack of data in Blocks 1 and 2 (Table B.3). Limit switches on the armatures malfunctioned on both AFTS after Block 10 (J-occlusion extension at Unit 4-2) and Block 11 (upstream of Unit 4-1). The AFTS upstream of Unit 4-3 was repaired and redeployed with slightly different operational features in order to sample the occluded treatment in Block 12 until the end of the study. Overall observations were made with the J-occlusions IN and OUT.

Table B.3. Summary of Sonar Tracker Data Collection by Study Location, Date, and Time Block when Data Were Collected at TDA in 2002. A total of 37,937 fish were tracked.

AFTS Location	Block	Dates	J-Occlusions	No. Day Tracks	No. Night Tracks
Unit 4-2	1	20-April to 23-April	IN	NO DATA	
J-Occlusion	2	26-April to 29-April	IN	NO DATA	
Extension	3	5-May to 8-May	IN	1189	745
	4	8-May to 11-May	IN	2377	915
	5	14-May to 17-May	IN	718	542
	6	23-May to 26-May	IN	1546	579
	7	29-May to 1-June	IN	1674	904
	8	4-June to 7-June	IN	511	412
	9	7-June to 10-June	IN	694	318
	10	13-June to 16-June	IN	354	173
	11	22-June to 25-June	IN	Instrument Malfunction	
	12	28-June to 1-July	IN		
	13	4-July to 7-July	IN		
	14	10-July to 13-July	IN		
Total				9063	4588
Unit 4 – Unit 5	3-11	1-May to 22-June	IN	5269	1288
Piernose			OUT	4386	2377
	12-14	28-June to 13-July	IN	5585	2211
			OUT	2669	501
Total				17909	6377

Data analysis to test the effect of the J-occlusion at the edge of the J-occlusion extension at Unit 4-2 in the context of a formal experimental design will not be appropriate because there was no corresponding volume of data for the unoccluded treatment. The data from AFTS deployed at the piernose between Main Units 4 and 5 were taken from a different sampling volume. However, we do have overlapping observational “periods” for the J-occlusion plates removed (MU 4-2) and deployed (piernose) conditions (Table B.3). The operation of the piernose AFTS was somewhat sporadic due to errors in a control program; therefore, the data was not organized by block, but as two periods - the additional features of day and night. At the MU 4-2 J-occlusion extension the data were organized into blocks and a depth distribution analysis was performed by block. For fish fate analysis, succeeding two blocks were

combined for comparison purposes (Blocks 3 and 4, Blocks 5 and 6, Blocks 7 and 8, and Blocks 9 and 10). Thus in summary, there are three “analysis factors” that can be examined qualitatively:

1. Time “block”
2. Day/Night
3. IN/OUT.

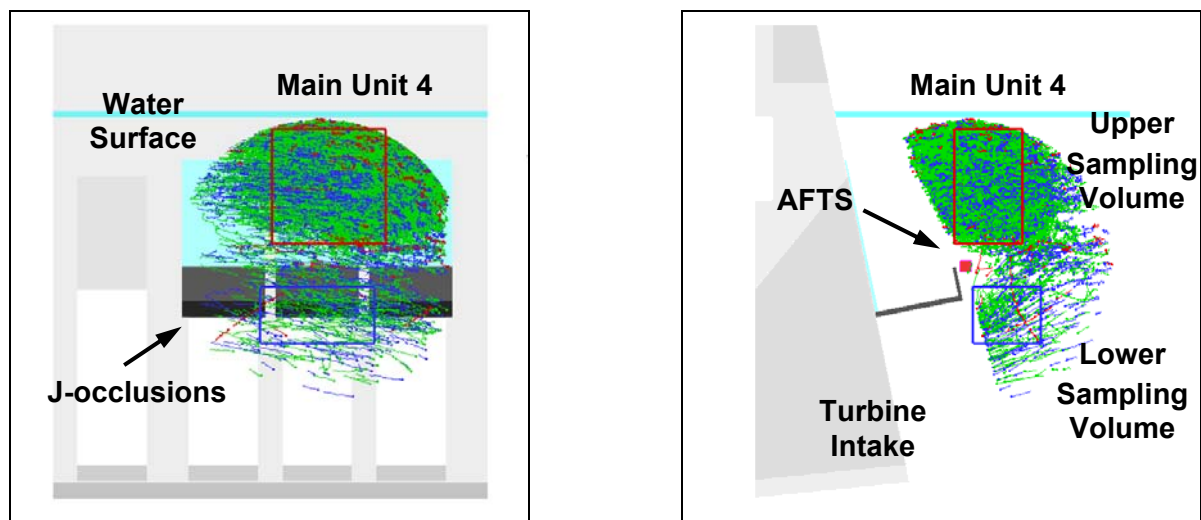


Figure B.3. Side and Front Views Showing Unit 4 with J-Occlusions Deployed. The blue, green, and red lines portray the fish tracks and sample volumes are represented by the red and blue boxes used in Markov-chain analysis.

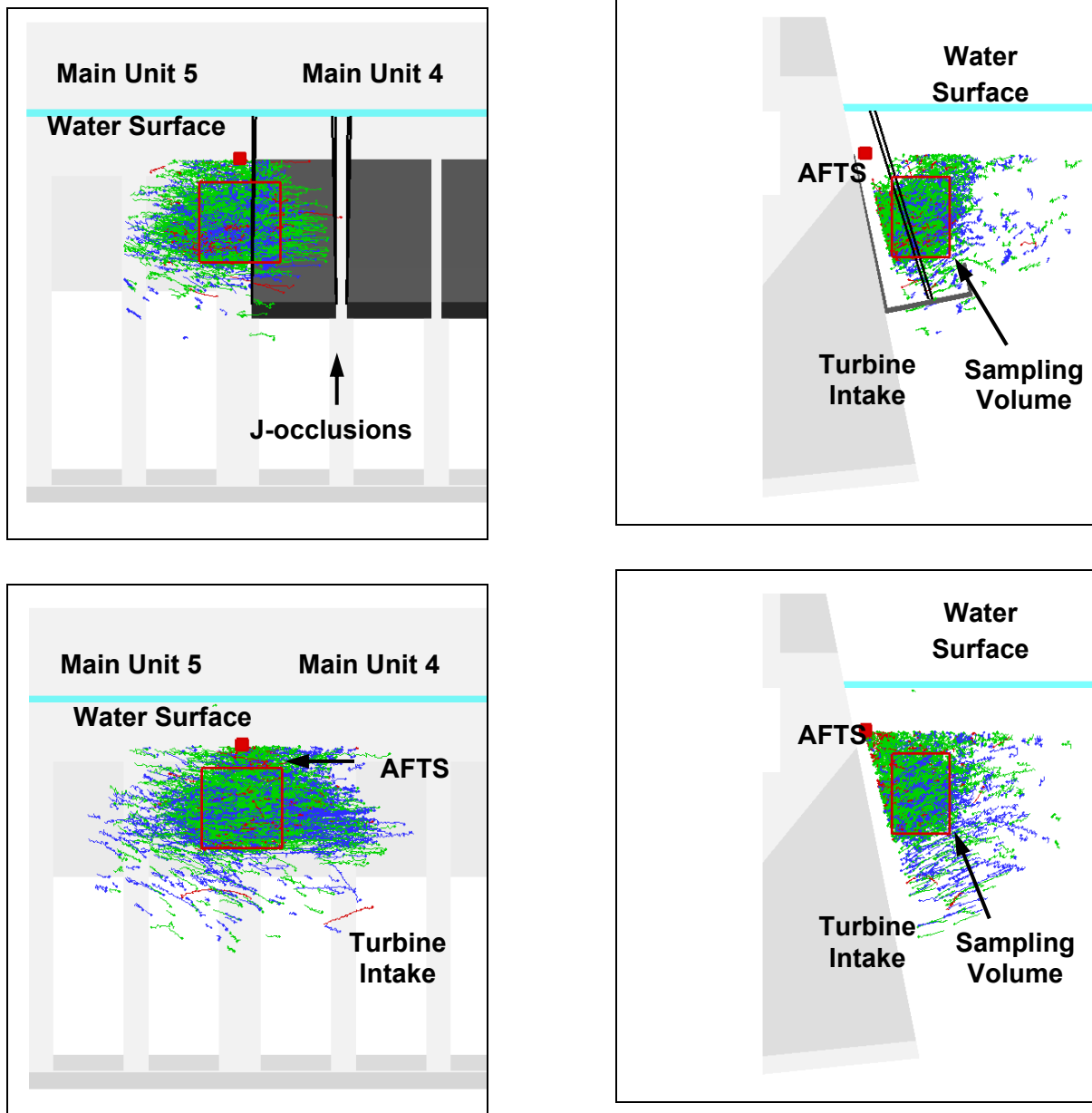


Figure B.4. Side and Front Views Showing Units 4 and 5 with J-Occlusions Deployed (top) and Removed (bottom) with Fish Tracks and Sample Volumes Used in Markov Chain Analysis. Figures show time period May 1 to June 22, 2002.

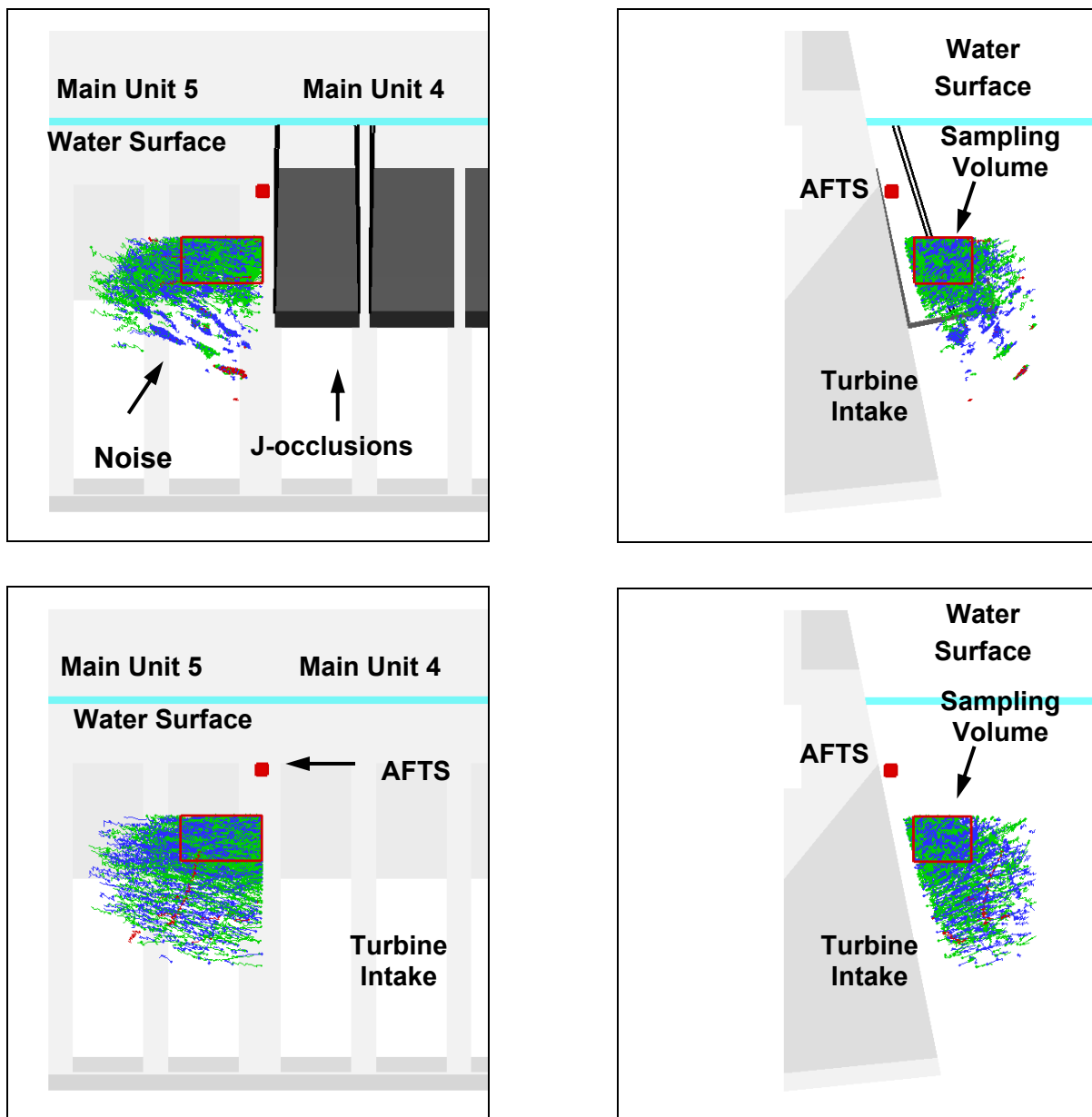


Figure B.5. Side and Front Views Showing Units 4 and 5 with J-Occlusions Deployed (top) and Removed (bottom) with Fish Tracks and Sample Volumes Used in Markov-Chain Analysis. Figures show time period June 28 to July 13, 2002.

B.2 Data Reduction and Analysis

Data reduction and analysis steps are described in this section. (See Hedgepeth et al. 2002 for a detailed flow diagram.) Although hydraulic data are available, the analysis included only observed fish movement data. Typically, day and night periods (see definitions below) were analyzed separately because of known day/night differences in sluice passage (Ploskey et al. 2001).

The tracking data from AFTS (TXT files) were filtered for minimum number of echoes per track (10) using a C-compiled program called TRKPROCA.EXE. The TRA output files from this program were reduced in a SAS-program called EDITQC.SAS, which removed unnecessary auxiliary information. The daily output files from the editing process were called TR1 files.

The daily TR1 files were edited to removed data in the four-hour period from 0800 to 1200 on days when the J-occlusions were changed. The edited TR1 files were concatenated into either experimental blocks or study periods. The resulting and the daily TR1 files were processed using a C-compiled program called TIP3D.EXE. Two daily block or period output files were produced: DAT files formatted to be loaded into Tecplot software (Amtec Engineering, Inc. Bellevue, Washington) and TEC files for further data and statistical analysis.

B.2.1 Data Processing

Data processing by TIP3D included:

B.2.1.1 Reassemble Tracks

Separate tracks adjacent in time and space were reassembled. This usually occurred when AFTS automatically broke off tracking when the maximum number of echoes per track was reached (800) or when the maximum number of missing pings was reached (20).

B.2.1.2 Fish Track Identification Number

The purpose here was to give each track a unique identification number for subsequent data analysis. A fish track identification number was made from the date and an integer starting at 1 and proceeding consecutively.

B.2.1.3 Day/Night Determination

Sunrise and sunset times for each date during the study period were obtained from the U.S. Naval Observatory website (http://aa.usno.navy.mil/data/docs/RS_OneYear.html) using the latitude and longitude of the reservoir (45°37'N 121°08'W). The time of the start of a given fish track was then compared to the sunrise/sunset times to determine if the track was in day or night. A day/night designator was then written to the output file: day = 0 and night = 1.

B.2.1.4 Delta X, Y, Z, T Calculations

The difference in three-dimensional fish position (X, Y, Z) and time between consecutive echoes in a track was calculated as follows, using delta X as an example between the i and i+1 echoes of the track:

$$\Delta X = X_{i+1} - X_i$$

B.2.1.5 Conversion to Dam Coordinates

The raw position data are in “tracker” coordinates, i.e., relative to the location of AFTS’s split-beam transducer and rotators (centered at intersection of axes). This Cartesian coordinate system was converted to “dam” coordinates for the purposes of display and analysis. The origin of the “dam” coordinate system was the center of the MU1-1/FU2-2 pier nose at Elevation 48.2 m (158 ft).

B.2.1.6 Conversion to Oregon State Plane Coordinates

Similarly, the raw position data were also converted to Oregon State Plane NAD 27 coordinates. This is the same coordinate system that other researchers and CFD modelers will use.

B.2.1.7 Tecplot Visualization

We used Tecplot software to visualize the fish tracks obtained from AFTS. To do this, we first rendered the dam in Tecplot. Then the specific tracks contained in the DAT files from the TIP3 programs were turned into “zones” in Tecplot. The tracks were superimposed on the dam rendering, both of which were in “dam” coordinates. Tecplot visualization allowed us to manipulate and explore the three-dimensional nature of the tracks relative to the dam.

B.2.1.8 SAS Descriptive Data

Descriptive data on the data set were obtained using the SAS-program DESCRIP.SAS. Using the TEC files as input, DESCRIP.SAS produced the following data for each day/night period in each treatment:

- number of observations (distinct fish positions);
- mean, minimum, and maximum number of echoes per track;
- mean, minimum, and maximum positions in the X, Y, and Z dimensions;
- mean, minimum, and maximum velocities in the X, Y, and Z dimensions.

B.2.2 Analyses

B.2.2.1 Velocity Vectors and Streamtrace Analysis Based on Ping-to-Ping Estimated Velocities

Ping-to-ping velocity data averaged within each 1.0 m cell were the basis for the mean velocity analysis at both AFTS (MU 4-2 and piernose at MU 4-MU 5) and a streamtrace analysis for the AFTS at MU 4-2. Mean velocities over the entire sample volumes (Table B.4) were obtained for each study period for each dimension (X, Y, and Z) for day and night separately. Using the base data set of mean X, Y, Z velocities by 1.0 m cell, streamtraces were generated using an interactive steamtrace tool in Tecplot for X/Y and Y/Z velocity vectors separately. All subsequent data analyses were based on fish track data, not ping-to-ping data.

B.2.2.2 Direction of Movement Based on Identified Fish Tracks

Fish track directionality relative to the presence of J-occlusions, night versus day and spill condition, can be characterized using proportions based on individual track regressions in each of the three dimensions: along the dam, upstream/downstream, and up/down. The movement proportions were based on the results of linear regressions applied on each fish track for each dimension separately to estimate three components of movement. All tracked fish in each data set were used from the entire sample volume with the exception that only fish tracks with mean depths less than 14 m were used from the piernose tracker due to noise in the deeper data when the J-occlusions were deployed. Proportions of fish moving in each of three dimensions were calculated for each cell. These movement proportions were then the basis for a comparison of movements with and without J-occlusions in place. Summary mean proportions were tabulated for direction of movement separately for each dimension.

B.2.2.3 Markov Analysis of Fates Based on Identified Fish Tracks

For the purpose of this study, a fate is specified by where fish tracks exited the sample volume. Fates are expressed as probabilities of passage toward a particular area, e.g., the sluiceway. To determine fate probabilities, we applied a Markov analysis (Taylor and Karlin 1998, pp. 95-266), which described smolt movement as a stochastic process. Two key ideas from Taylor and Karlin (1998, pp. 95-96) are: (a) a Markov process $\{X_t\}$ is a stochastic process with the property that, given a value X_t , the values of X_s , for $s > t$ are not influenced by the values of X_u for $u < t$, and (b) transition probabilities are functions not only of the initial and final states, but also of the time of transition as well. When the one-step transition probabilities are independent of the time variable, then the Markov chain has stationary probabilities. The Markov-chain analysis for the 2001 TDA sonar tracker study included the following assumptions.

- The movements can be described by a one-step Markov process. In other words, movement decisions are based on the smolt's current position and not upon the prior history getting to that position.
- The transition probabilities are estimated from independent fish observations.
- The transition matrix is stationary.

The three-dimensional sample volumes in front of Units 4 and 5 were divided into cells (modified for fate analysis as follows: 1.0 x 1.0 x 1.0 m for X, Y, Z, respectively). The sample volume was decreased to include a large number of tracks in each cell (Table B.4). At the boundaries (sides) of the volume, we defined these passage fates:

- Up – cells on side facing the surface
- Down – cells on side facing the bottom
- Dam – cells on side facing the dam
- Reservoir – cells on side facing the reservoir (upstream)
- West – west side cells
- East – east side cells
- Unknown – no movement or not absorbed into a boundary.

Table B.4. Number of 1.0 m X 1.0 m Cells in Sample Volumes for Markov Analysis. The number of cells is equal to the number in X (along dam) times Y (horizontal perpendicular to dam) times Z (up-down).

Location	Period	Volume	J-Occlusions	Number of X Y Z Cells	Interior Cells
J-extension Unit 4-2	May 5 to June 16	Upper	IN	11 X 8 X 10 = 880	432
		Lower	IN	10 X 6 X 5 = 300	96
Piernose between Unit 4 and Unit 5	May 1 to June 22		IN, OUT	7 X 5 X 7 = 245	75
	June 28 to July 13		IN, OUT	7 X 5 X 4 = 140	30

The Markov transition matrix was a square matrix the size of $k \times k$, where k is the number of distinct cells being modeled. The ij th element in the i th row of the j th column of the transition matrix was the estimated probability (p_{ij}) of moving from cell i to cell j in the next time step. These probabilities were estimated by:

$$\hat{p}_{ij} = \frac{x_{ij}}{n_i}$$

where

n_i = number of observations of smolts in the i th cell;

x_{ij} = number of observations where a smolt in cell i moved to cell j in the next time step.

The cells (1.0 x 1.0 x 1.0 m) that bordered the sides of the volume of interest (dam, top, west, east, bottom, and reservoir) were set to unity to absorb any movement that reached a particular "fate." Otherwise, the C-compiled program FATE.EXE tallied the transition matrix T using a time step of 0.5

sec, and the average position (i.e., $\frac{\sum x_i}{n}$) during each 0.5 s interval a fish was tracked. This program required that a fish be tracked for at least two seconds before the transition matrix was amended to obtain indices i and j (i from the first interval, j from the second). Non-boundary (including surface) cells were checked to ensure non-zero and non-unity values. If zero or unity was present in an i, i cell after building the matrix T from a set of data, then the closest i, i cell in Cartesian space was found that contained data and was used to augment that particular set of i, j 's. This process created a situation that guaranteed fish movement to one of the absorbing boundaries if there was movement to begin with.

The transition matrix T for one time step was then used to estimate the transition for two or more time steps as:

$$T^t$$

where, t = the number of time steps. For this study, $t = 2^{50}$ so that the Markov process reached stability, i.e., the transition matrix did not change with additional time steps. The ultimate fate of smolts would be calculated as:

$$T^{2^{50}}.$$

After 2^{50} time steps, probabilities for each of the seven fates for each of the interior cells (i.e., not including border cells) were extracted from the transition matrix and written to file. The fate data were displayed in Tecplot.

The key assumption in this analysis is that the data exhibit the Markov property (see first assumption above). The one-step model we used in the analysis of day and night fish movement assumed movement to a future cell depended entirely on the fish's current position, not its prior history. However, movement could depend on both the current and past histories. A $R \times C$ table was used with data collected at The Dalles Dam in 2001 to test whether movement from B to C_i is independent of previous position A_i .

The data presented in the final report of the sonar tracker evaluation of fish movements in 2001 (Hedgepeth et al. 2002) were re-tested using the SAS Exact option (SAS Institute Inc. 1990). As many cells as were practical were tested in this manner. Movement and cells were measured using a time step of 0.5 s and 1.0 m per side cells with x values indexed i ($i=0 \dots M$), y values indexed j ($j=0 \dots N$), and z values indexed O ($k=0 \dots O$). Cell codes were formed as $i+j*M+k*N$. An asymptotic chi-square test was not used due to sparseness of the contingency tables. Therefore, conclusions about appropriateness of the first order assumption of a one-step Markov process will be based on Fisher's exact test (Mehta and Patel 1983).

The contingency analysis was performed on two conditions: Plates In, Day, No Spill and Plates In, Night, No Spill. During the daytime the Fisher Test showed 5% of 268 tests were significant at the 0.05 level (and 11% at the 0.1 level). At night, 6% of 766 tests were significant at the 0.5 level (and 11% at the 0.1 level). Figure 6 shows plots of the significance probabilities. They do not show uniformity because of larger frequencies in the 0.95 to 1.0 significance bin.

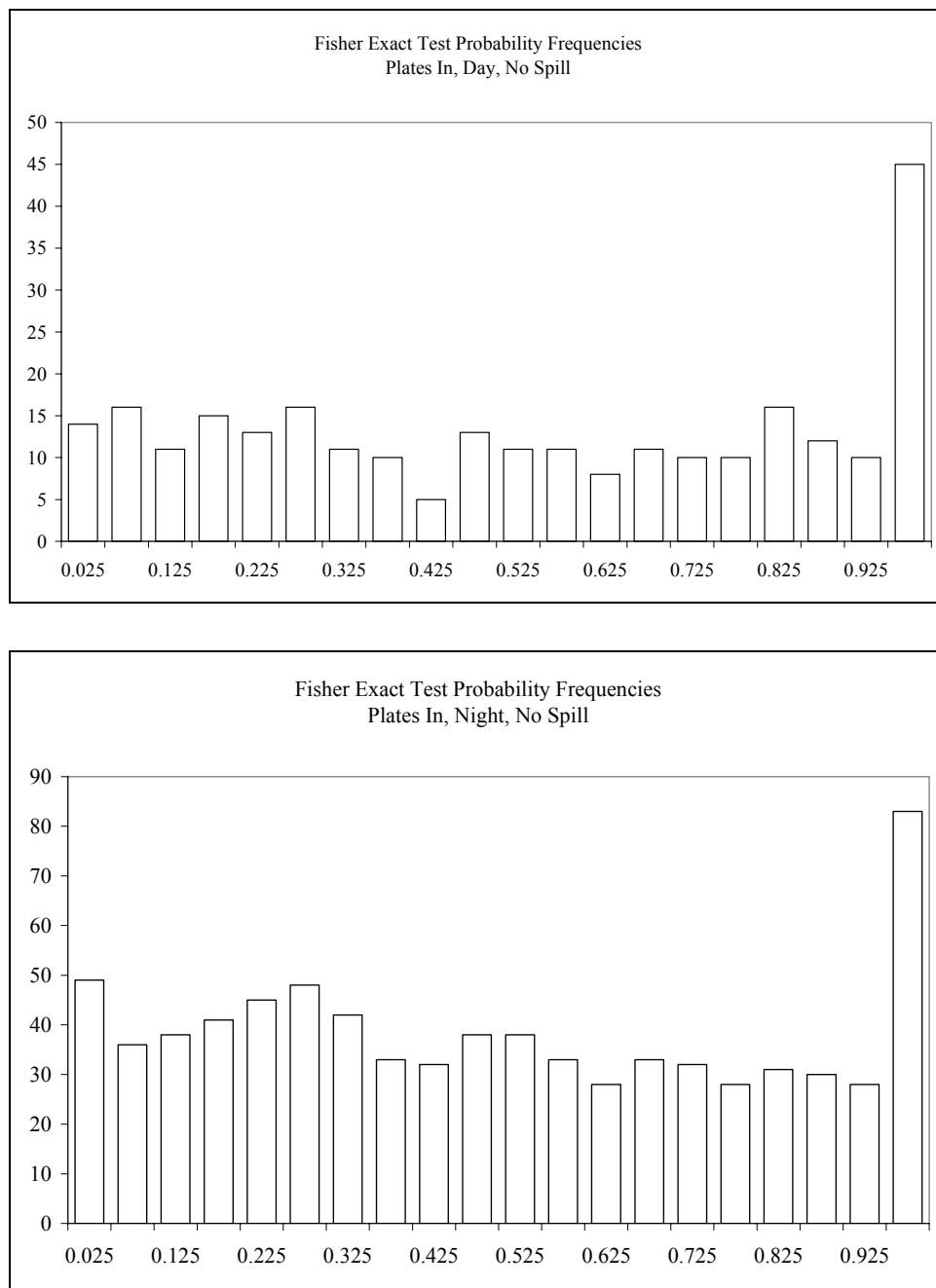


Figure B.6. Plots of Significance Probabilities from Fisher Exact Tests on Independence of Movement with Past Movement. Data is from TDA 2001. Above: J-occlusion plates in, day, no spill. Below: J-occlusion plates in, night, no spill.

In addition to comparing fish movements in general for various conditions, we are interested in assessing the edge effects of the J-occlusions on fish movements near Main Unit 4. We used the fate probabilities from the Markov-chain analysis to calculate “probability indices.” A probability indices (PI)

for a given condition will simply be the average fate probability over all cells in the sample volume, as follows:

$$PI = \frac{\sum_{i=1}^m \sum_{j=1}^n \sum_{k=1}^o F_{ijk}}{m \cdot n \cdot o}$$

where, F_{ijk} is the fate probability for the i th cell along the dam the j th cell away from the dam, and the k th cell deep.

In addition, we calculated the volume ($VTOT_{PI}$) where the fate probabilities were equal to or greater than 0.1, 0.3, 0.5, 0.7 and 0.9, as follows using 0.7 as an example:

$$VTOT_{0.7} = V_{cell} \sum_{i=1}^p \sum_{j=1}^q \sum_{k=1}^r F_{ijk}$$

where, $F_{ijk} \geq 0.7$ and V_{cell} is the volume per cell.

B.3 Vertical Distribution

The fish vertical distribution on the reservoir side of Unit 4-2 J-occlusion was estimated using weights equal to the reciprocal of volumes of vertical slices of the AFTS sampling volume. A sphere surrounding the AFTS to 13 m, with intersecting limiting planes and two obscured conical regions, formed the sampling volume. The upper hemisphere's limiting plane intersected the AFTS position, paralleled and tilted toward the dam face at 25° from vertical. The lower hemisphere's limiting plane intersected the AFTS position, paralleled and tilted away from the dam face at 15° from vertical.

Analytical and numerical integration methods were used to approximate sampling volumes in 1-m depth bins. The volume of the front half of a hemisphere from depth z_1 to z_2 is

$$\begin{aligned} \text{Volume}_{\text{Half-Hemisphere}} &= \int_{z_1}^{z_2} \frac{1}{2} (13^2 - z^2) dz \\ &= \frac{1}{2} \pi \left[13^2 (z_2^2 - z_1^2) + \frac{1}{3} (z_1^3 - z_2^3) \right]. \end{aligned}$$

A volume that resulted from a plane that intersected the sphere was approximated using the mid-interval depth times the area of a circle segment. This volume was either added (upper hemisphere) or subtracted (lower) from the half-hemisphere slice. The volume of a circle segment can be calculated as a function of depth z and angle Θ from vertical as

$$\text{Volume}_{\text{Segment of Sphere}} \approx \Delta z \text{Area}_{\text{Segment of Circle}}$$

$$\approx \Delta z \frac{1}{2} (13^2 - z^2) \left[\pi - 2 \cos^{-1} \left(\frac{z \tan \theta}{\sqrt{13^2 - \Delta z^2}} \right) + \sin \left(\cos^{-1} \left(\frac{z \tan \theta}{\sqrt{13^2 - \Delta z^2}} \right) \right) \right]$$

where $\Delta z = z_2 - z_1$ and $z = \frac{z_2 + z_1}{2}$.

A conical volume obscured part of the spherical sampling volume because the inner armature of AFTS moves only to $\pm 62^\circ$. This volume was estimated as Δz times the area between a hyperbola and the circle at a level z , using Mathematica (Wolfram Research),

$$\text{Volume}_{\text{Planar Cone Slice}} \approx \Delta z \text{Area}_{\text{Planar Cone Slice}}$$

The area was found between a circle and a hyperbola by integration and a 3rd order polynomial was fit to the volumes as a function of z

$$\text{Volume}_{\text{Planar Cone Slice}} \approx \Delta z (0.4467z^3 - 4.6449z^2 - 2.1038z + 82.813)$$

The sampling volume above the elevation of AFTS was

$$\text{Volume}_{\text{Half Hemisphere}} + \text{Volume}_{\text{Segment of Hemisphere}} - \text{Volume}_{\text{Planar Cone Slice}}$$

and the sampling volume below the elevation of AFTS was

$$\text{Volume}_{\text{Half Hemisphere}} - \text{Volume}_{\text{Segment of Hemisphere}} - \text{Volume}_{\text{Planar Cone Slice}}$$

Fish tracks with a minimum of 10 pings per track were used to establish fish depth distributions. Each ping was counted as 1/(pings in track) and placed into a 1-m depth bin. The resulting distributions divided by the sampling volume (shown in Figure B.7) formed estimated fish depth distributions. Distributions were reported by experimental block and day/night.

Confidence intervals (CI) were estimated by bootstrap resampling (Efron and Tibshirani 1993). A CI resulted by adding and subtracting, from the mean depth, two times an estimate of the standard error of the mean. The estimate of SE used 1,000 bootstrap samples (i.e. sampling with replacement) of the estimated distributions, scaled so that $n = 10,000$. Depths used in bootstrap resampling were the mid-depth of a bin. Bootstrap samples were performed using S-Plus v 4.5, using the function: bootstrap (Depths, mean, B=1000).

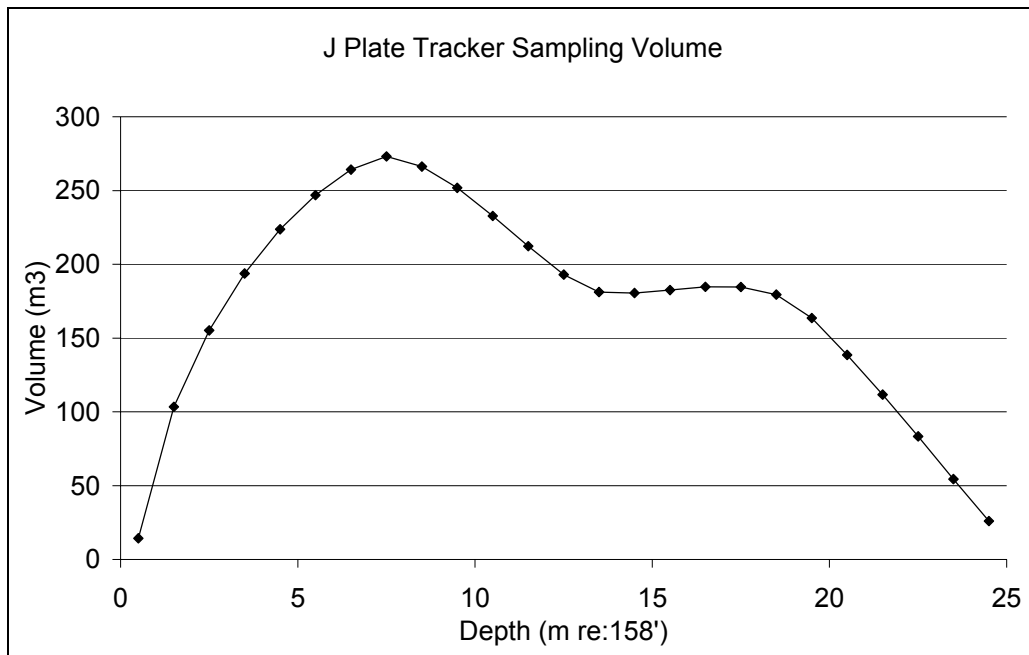


Figure B.7. Sampling Volume as a Function of Depth of AFTS Located on the J-Extension Plate of Main Unit 4-2. Line shows volume in cubic meters per meter of depth.

Appendix C: DIDSON Methods

Appendix C

DIDSON Methods

C.1 Description

The Dual-Frequency Identification Sonar (DIDSON) was developed by the Applied Physics Laboratory (APL) at the University of Washington for the Space and Naval Warfare Systems Center harbor surveillance program (Belcher et al. 1999). It can detect objects out to 48 meters and provide near video-quality images to identify objects out to 8 meters. DIDSON was designed to bridge the gap between existing sonar, which can detect acoustic targets at long ranges but cannot record the shapes or sizes of targets, and optical systems, which can videotape fish in clear water but are limited at low light levels or when turbidity is high. DIDSON has a high resolution and fast frame rate designed to allow it to substitute for optical systems in turbid or dark water. The $7 \times 12 \times 8$ -in. unit weighs only 15 lbs in air.

A near photographic image clarity is possible because the field of view is composed of 96 different 0.3-degree beams operating at 1.8 MHz with a 29-degree field of view. The multiple beams allow image processing that produces a near-field image similar to that of a CCD video camera. Unlike single and split-beam hydroacoustic transducers, the acoustic camera has multiple narrow beams that allow it to be aimed oblique to a flat surface and still record fish swimming very near the water's surface or a solid surface (Figure C.1). For this study, the DIDSON was primarily used in the high frequency mode at a frame rate of 7 frames/s. Data files were saved to an external hard drive with separate data files generated sequentially at 10-min intervals.

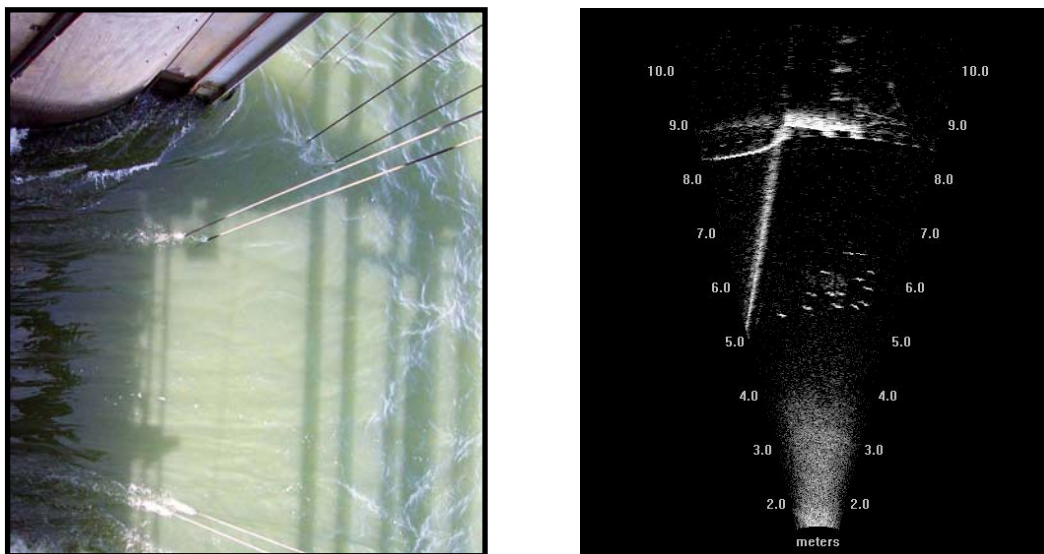


Figure C.1. Optical View of the Ice and Trash Sluiceway (left) and DIDSON Acoustic View of the Ice and Trash Sluiceway (right). Details in the acoustic image include the trashrack guide slot and trashrack, piernose, occlusion guide slot, and smolts approaching the entrance.

C.2 Deployment

The DIDSON was mounted to a custom aluminum trolley that was lowered on a steel I-beam which was welded to the J-plate guide frame at the main pier nose of MU 1-2 and 3-4. The section of I beam on unit 1-2 extended down to the floor of the J-plates (el. 105) and the section 3-4 extended down to an elevation of 85 ft. The trolley was raised and lowered using an electric winch hoist along with a davit. An underwater 3-axis rotator (R.J. Electronics PTE-200 and R-200) was mounted to the trolley and the DIDSON was fastened at the single axis rotator to allow for full range of movement. This instrument allowed us to position the DIDSON array with relatively high accuracy ($\pm 1^\circ$ azimuth) on the pan, tilt, and rotate axes. The aiming angles (in degrees) from the rotator were also incorporated into the DIDSON program using a Serial Data Acquisition Module. This allowed feedback from the rotator individual axis to be associated with each DIDSON frame. Figures C.2 and C.3 show the forebay and plan views of DIDSON's coverage zone.

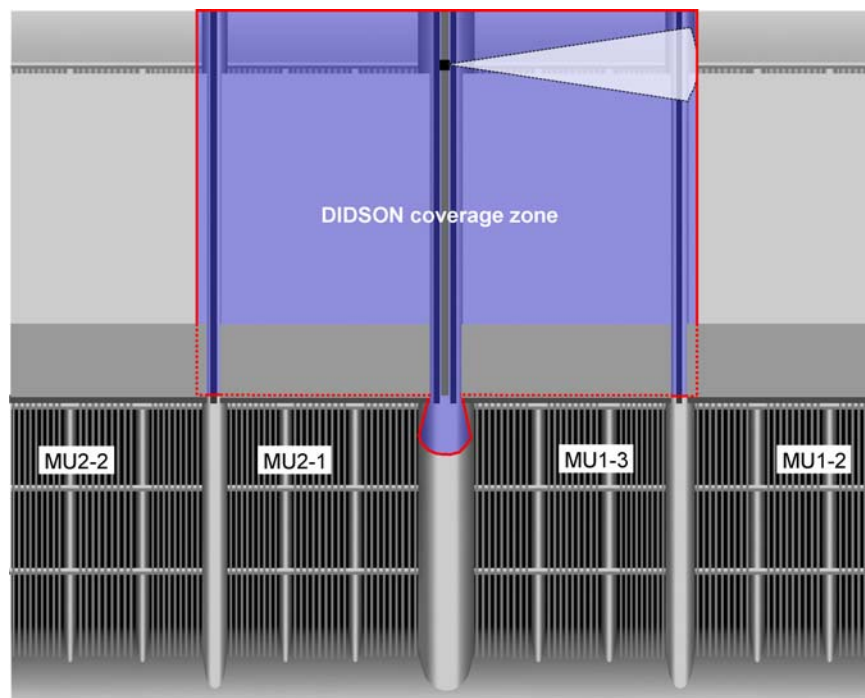


Figure C.2. Forebay View of the Sampling Volume

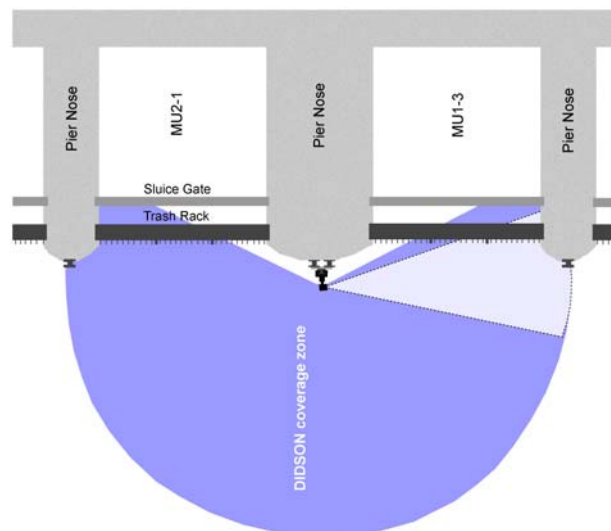


Figure C.3. Plan View of Sampling Volume

C.2.1 Sampling Schedule

The sampling for the spring and summer study was split between the two deployment locations at MU 1-2 and 3-4. This research use of the DIDSON was coordinated with other Corps research projects. The sampling dates from April 26 to May 15 and from June 19 to July 12 were assigned prior to the field season to this project. The sampling duration was fairly evenly split between the spring (21-day) and summer (23-day) period.

A scanning regime was used to detect the presence of predators at each location. This regime consisted of both fixed positions and active scans. This required a human operator to be present during the scans. Based on early observations, these intensive scanning periods were restricted to the diel peaks of fish occurrence from 0500 to 1000h and from 1700 to 2200 h (Table C.1).

Table C.1. Scan Positions for DIDSON Deployed at Pier 1-2

Position	Duration	Sampling Zone
1	10 min	Inner portion of sluiceway
2	10 min	Just outside of 1-3 plate/trashrack
3	10 min	25-30° out from 1-3 plate/trashrack
4	10 min	Just outside of 2-1 plate/trashrack
5	10 min	25-30 deg out from 2-1 plate/trashrack
6	Scanning	Vertical scan along 2-1 plate
7	Scanning	Horizontal scan from plate 1-3 to 2-1. Vertical scan along piernose.
8	Scanning	Vertical scan along 1-3 plate

Table C.2. Scan Positions for DIDSON Deployed at Pier 3-4

Position	Duration	Sampling Zone
1	10 min	J-extension gap near tip of J
2	10 min	J-extension gap near piernose
3	3 min	Straight out
4	3 min	Left of piernose
5	3 min	Right of piernose
6	Scanning	Vertical scan along 4-1 plate/trashrack
7	Scanning	Vertical scan 25 deg away from plate/trashrack
8	Scanning	Vertical scan along 3-3 plate/trashrack
9	Scanning	Vertical scan 25 deg away from plate/trashrack

C.2.2 Sampling Effort

Due to the reconciliation of the study block schedule and DIDSON availability, sampling did not occur equally between J-occlusion treatments (Figure C.4). Rather than reducing the dataset to the shortest common sampling period, rates of detection were used in further analyses.

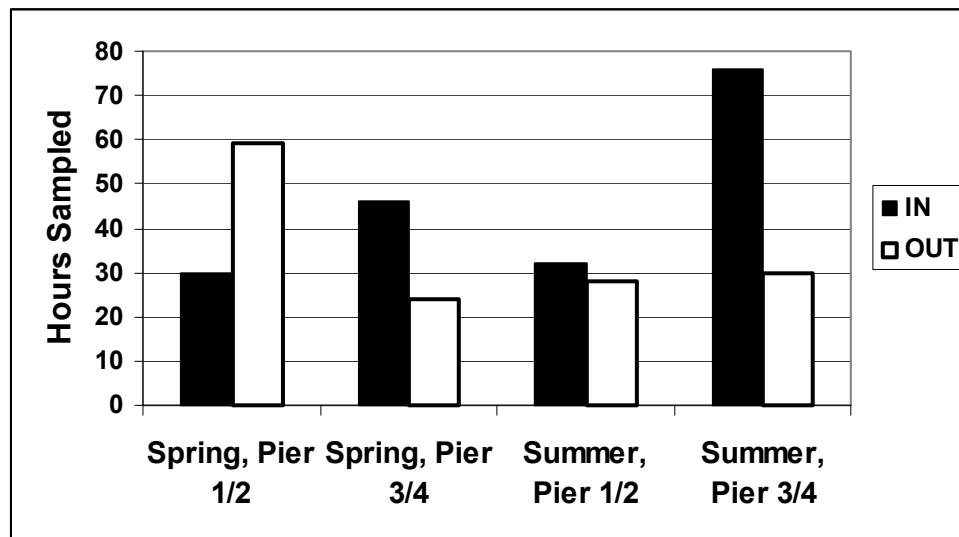


Figure C.4. Sampling Duration in Hours at Each Location (Pier 1/2 or 3/4), Season (spring or summer), and Treatment (J-occlusions IN or OUT)

Appendix D: Comments on Draft Final Report and Responses

Appendix D

Comments on Draft Final Report and Responses

Formal comments on the Draft Final Report dated January 10, 2003, were received from Dr. Cliff Pereira of Oregon State University. Those comments are reproduced below. Our responses to the comments are inserted in **Arial bold** font.

DRAFT MEMO

February 13, 2003

TO: Dan Feil

FROM: Cliff Pereira

RE: Comments on the Final Draft report: Hydroacoustic Evaluation of the J-Occlusion Plates at The Dalles Dam in 2002 by Johnson, et al.

Lots of good graphics and well-organized.

Page 5.1 Figure 5.1. Because it is difficult to see the smaller numbers (note all the white space), may want to use a log scale. Could also show blocks with dashed vertical lines.

Agree. We decreased the range on the Y-axis, changed the color of the SMP data line so that it showed when printed, and added dashed vertical lines to show the blocks.

Page 5.3, 5.1.3 passage by block. The graphics are effective in showing that only for total passage in the summer (both day and night) are there consistent differences between the IN and OUT treatments. We will come back to the graphics in a moment.

Response not necessary.

Page 5.6, 5.1.4 Statistical Comparison. Table 5.1 has some problems, fortunately once it is corrected, the conclusions will not change. My first hint that I should look closer were the two extremely small F-values (<0.001). It is well-known amongst experienced applied statisticians that “whenever we see a significantly small F statistic, it should give us pause (Christensen (2003)).” Is an F-value <0.001 “significantly small?” For Day, the F distribution has d.f. of 1 and 6, so that an F-value <0.001 has a p-value >0.992 . This means that less than 8 times out of 1000 would we expect to get an F-value that small or smaller.

Agree. We re-checked the ANOVA and found an error in the data being used to calculate the error sum of squares. This mistake resulted in exceedingly low F-values. The correct F-values range from 0.4 to 13.7. The ANOVA data were corrected accordingly.

Fortunately I do not need to fully explain this issue because the most recent issue of American Statistician (February 2003) has a very nice exposition on the issue by Ron Christensen, an expert on linear models. Because it is in American Statistician, it is a very readable article with lots of examples to show how “Significantly Insignificant F Tests” may be an indication of an

incorrect model for the data. The basic idea is that under the model for the null hypothesis, the p-value has a uniform zero-to-one distribution, so that p-values very close to one are just as unlikely as p-values very close to zero. Here is the abstract for the article:

Title: Significantly Insignificant F Tests

Author(s): Ronald Christensen

Source: The American Statistician **Volume:** 57 **Number:** 1 **Page:** 27 -- 32

DOI: 10.1198/0003130031108

Publisher: American Statistical Association

BEGIN ABSTRACT: P values near 1 are sometimes viewed as unimportant. In fact, P values near 1 should raise red flags cautioning data analysts that something may be wrong with their model. This article examines reasons why F statistics might get small in general linear models. One-way and two-way analysis of variance models are used to illustrate the general ideas. The article focuses on the intuitive motivation behind F tests based on second moment arguments. In particular, it argues that when the mean structure of the model being tested is correct, small F statistics can be caused by not accounting for negatively correlated data or heteroscedasticity; alternatively, they can be caused by an unsuspected lack of fit. It is also demonstrated that large F statistics can be generated by not accounting for positively correlated data or heteroscedasticity.

Response not necessary. This is a moot point.

As I looked at the data, I wondered if the F -value really was that small. Estimating the data from the graph, my approximate F -statistic for a randomized complete block design (here equivalent to a paired t -test) was 1.05 for Spring Day MU1-4 passage with a p -value = 0.354 and 0.55 for Spring Night MU1-4 passage with a p -value of 0.49. These I suspect are much closer to the correct F -values than the <0.001 listed in the table.

Agree. See response immediately above.

The tables would be much more informative if they contained p -values rather than, or in addition to, the F -values. The table gives a cutoff, but this is insufficient information and it is incorrectly stated. Only one cutoff is given, yet the spring test has 1 and 6 d.f. while the summer test has only 1 and 5 d.f. Therefore, if cutoffs are used at all, there would need to be two cutoffs: 5.99 for Spring and 6.61 for summer. The sentence would not talk about 95% confidence level, but rather significant at the $\alpha = 0.05$ level. However, much more important than the cutoff are the actual p -values.

Agree. We deleted Table 5.1 and added F -values and P -values for the $\alpha = 0.05$ level to the block data (Figures 5.3, 5.4, and 5.5).

Personally, I would take each graph and first place a vertical dashed line between blocks 7 and 8 to demark the changeover from spring to summer. Second, I would add under the set of spring blocks in each graph the F -value and p -value ($F=1.05$, p -value=0.354). I would also add the F -value and p -value under the set of summer blocks on the graphics. Why force the reader to flip back and forth between the table and the graphics?

Agree. See response immediately above. Also, we added lines delineating spring and summer in Figures 5.3, 5.4, and 5.5.

If the table is kept, it might look something like:

	Spring		Summer
MU 1-4	Day	Night	Day
	F=1.05	F=0.55	etc.
	(p=0.35)	(p=0.49)	

etc.

Non-applicable. The table was deleted.

NOTE: The methods state that log transformations and the “arcsin transformation” were used. However, it should be made explicit what was done to each response, such as that counts were log transformed and metrics that must lie between zero and one were arcsin transformed. It is not clear if either transformation is really needed for much of the analyses, therefore it would be worthwhile to simply note in the methods that “Analyses of data on the original scale gave the same conclusions.”

Agree. We added an explanation to Section 3.2.3 Statistical Methods regarding which data were ln-transformed (MU 1-4 passage) and which were arcsin-transformed (sluice efficiency and FPE). We did not analyze untransformed data.

NOTE: The statistical methods section refers to a number of one-tailed tests. Yet the analyses appear to be based on two-tailed tests. That is fine, but should probably make some statement in the methods such as: “It was decided to use two-tailed tests, because...”

Agree. We modified each section to be consistent about the two-tailed testing that was performed.

Page 5.7 Figure 5.6 What periods of time is represented by the figure. Is this some sort of average over some period of time, or is this just one time period? The legend does not seem to indicate that. Since spring and summer are different with respect to at least passage, then spring and summer could also differ in the fish velocity plots. I am not sure what the blue lines are relative to the red velocity vectors.

Agree. We supplied the time period (May 5 to June 16, 2003), explained why spring and summer were not separated (not enough data), and noted that the blue lines are streamtraces in the figure caption.

Table 5.2 Is this information summed over both spring and summer? Were spring and summer compared so that it was clear that spring and summer are similar enough that they should be summarized over? Could show both spring and summer to indicate the similarity.

Agree. As above, we explained in the caption that there were not enough data to perform separate analyses for spring and summer.

Figure 5.9 Good to examine systematic changes with blocks. Were other variables examined in the same way?

Agree. Data on changes with blocks were presented for MU 1-4 passage, sluice efficiency, and FPE (see Section 5.21.3), although a trend line was not provided.

Figure 5.10. Is there some way to show whether unoccluded was consistently higher than occluded across blocks as well?

No, the DIDSON data were not plentiful enough for a block analysis.

Figure 5.12 Good to show predator and prey over time, but it would also be nice to see the plot that shows predator vs. prey with a correlation of 0.67.

Agree. We added that.

Appendix. Page A.9. It is stated that the “variance of estimator (9) can be expressed as follows:” when what follows is an estimator of the variance. Therefore, to be consistent with other descriptions, could state that “the variance of the estimator can be estimated as follows.” NOTE: Same problem on A.11 for equation (14), A.12 equation (16), A.13 equations (18) and (20), etc.

Agree. We made the appropriate edits throughout Appendix A.

It is very good that it is noted that the “variance formula (9) [actually (10)] will likely underestimate the true variance because it does not take into account the variation in smolt passage between entrances.” This should be considered in future designs because this underestimation could be fairly large. Should probably be noted again in the results, because no one will probably read it buried here.

Agree. We added this point to the methods (Section 3.2.2.2).

Note: B.13. It is stated that “A Chi-square test was not used due to the sparseness of the contingency tables.” Note that sparseness does not invalidate the test statistic, just the Chi-square approximation for its distribution under the null. In SAS when one chooses the exact option, can get an exact p-value for the Pearson (Chi-square) statistic that is just as valid as the exact p-value for the Fisher’s exact test. So sparseness will lead one to use an exact test, but it is not a reason to choose between the Pearson exact p-value versus the Fisher’s Exact test p-value.

Agree. The Markov property assumption is that the probability of movement is independent of past history. We used an RXC Fisher exact contingency test to examine the validity of this assumption. We thank the reviewer for pointing out that exact p-value statistics are produced by other SAS RXC tests. PROC FREQ gives exact p-value statistics for Pearson’s chi-square, likelihood-ratio chi-square, Mantel-Haenszel chi-square, and Fisher’s exact tests. Fisher’s exact test was chosen because it is reported to be conservative. In the future, we will examine the exact p-values for Pearson’s chi-square and likelihood-ratio tests. We will change the text to say, “An asymptotic chi-square test was not used due to sparseness of the contingency tables.”

The description of the Markov analysis is good. I was not quite clear on the following. Does the testing refer to the one-step assumption only? Is there any way to test the stationarity assumption, by comparing something across some time periods within a season?

We tested the one-step assumption only. The stationarity assumption requires that transition probabilities remain the same over time. We did compare fate probabilities (a function of the transition probabilities) in four time periods as a function of day and night. The general outcome was similar for all four periods: high west probability, low east probability and some toward-dam and toward-turbine probability.

Another part of the stationarity assumption is homogeneity. We can test the homogeneity assumption by comparing different time steps. However, the nature of the data is that we have track lengths that are somewhat longer than the cell sizes used in the Markov-chain analysis. If we halve the time step (1 second) we would need to reduce the cell size, which will in turn make the estimation more time consumptive. If we double the time step, we reduce the amount of data that can be used.

